IC/89/50
INTERNAL REPORT
(Limited Distribution)

International Atomic Energy Agency
and
United Nations Educational Scientific and Cultural Organization
INTERNATIONAL CENTRE FOR THEORETICAL PHYSICS

THERMAL STRESS AND SEISMOGENESIS *

Zhou Huilan **
International Centre for Theoretical Physics, Trieste, Italy
and
Wei Dongping
Graduate School, University of Science and Technology of China,
P.O. Box 3908, Beijing, People's Republic of China.

ABSTRACT

In this paper, the Fourier stress method was applied to deal with the problem of plane thermal stress, and a computing formula was given. As an example, we set up a variate temperature field to describe the uplifted upper mantle in Bozhong area of China, and the computing results shows that the maximum value of thermal plane shear stress is up to nearly 7×10^7 P_a in two regions of this area. Since the Bohai earthquake (18 July, 1969, $M_s = 7.4$) occurred at the edge of one of them and Tangshan earthquake (28 July, 1976, $M_s = 7.8$) within another, their occurrences can be related reasonably to the thermal stress.

MIRAMARE – TRIESTE
May 1989

* To be submitted for publication.
** Permanent address: Department of Earth Sciences, Graduate School, University of Science and Technology of China, P.O. Box 3908, Beijing, People's Republic of China.

1. INTRODUCTION

When the temperature of elastic and constrained block changes, it would lead to an additional thermal stress field. By setting up regular and simple distribution of variate temperature field (VTF), some scholars once determined the force source and breeding mode of a number of earthquakes [1, 2, 3]. However, for the actual situation, we need a complex model of VTF, and then we have to adopt a numerical method to compute the thermal stress field. Based on the situation, we can make a further theoretical analysis on the general relations between thermal stress field and the VTF, and the cause of earthquake. For these reasons, in this paper, we apply the Fourier series method in the first section to deal with the problem of plane thermal stress which VTF distributes more generally, and give the theoretical computing formulas. Secondly, according to the analysis results based on the data of gravity anomaly, geomagnetic anomaly, thermal flow and seismic wave velocity, etc., we set up a plane VTF model that describes the uplifted upper mantle in Bozhong area of east China quite satsifactorily, and compute the thermal stress distribution in this area to approach the cause of Bohai (18 July, 1969, $M_s = 7.4$) and Tangshan (28 July, 1976, $M_s = 7.8$) earthquakes occurred there.

2. FOURIER SERIES SOLUTION OF PLANE THERMAL MODEL

For convenience, we give the definitions of symbols used in this paper.

- u: radial displacement;
- v: tangential displacement;
- σ_r: radial stress;
- σ_t: tangential stress;
- τ_{rt}: shear stress;
- ε_r: radial strain;
- ε_t: tangential strain;
- γ_{rt}: shear strain;
- α: coefficient of thermal expansion;
- E: Young's modulas;
- ν: Poisson ratio;
- $T(r,\theta)$: VTF function;

r and θ are radial and circular variables of polar coordinate system separately (see Fig.1).

Furthermore, we stipulate the superscript of these symbols as zero when $T(r,\theta)$ equals zero, i.e. the situation of no thermal influence, the superscipts as T when $T(r,\theta)$ nonzero but neglecting the pure elastic influence, and omitting the superscript when it is the sum of two situations.

2.1 Boundary Condition

Suppose all the components of displacement, stress and their corresponding boundary conditions can be expanded to Fourier series. The stress boundary condition around circle S meets

$$\sigma_r\big|_S = \sum_m (p_{cm}\cos(m\theta) + p_{sm}\sin(m\theta)) \tag{1a}$$

$$\tau_{rt}\big|_S = \sum_m (q_{cm}\cos(m\theta) + q_{sm}\sin(m\theta)) \tag{1b}$$

where p_{cm}, p_{sm}, q_{cm} and q_{sm} are all constants. Σ means sum.

2.2 Basic Equation of Thermal Stress Problem

Considering the medium of thermal model as elasticity, so the stress-strain relations of the thermal model satisfy

$$\varepsilon_r = (\sigma_r - \nu\sigma_t)/E + \alpha T \tag{2a}$$

$$\varepsilon_t = (\sigma_t - \nu\sigma_r)/E + \alpha T \tag{2b}$$

$$\gamma_{rt} = 2(1+\nu)\tau_{rt}/E \tag{2c}$$

and relations

$$\varepsilon_r = \frac{\partial u}{\partial r} \tag{3a}$$

$$\varepsilon_t = \frac{\partial v}{r\partial\theta} + \frac{u}{r} \tag{3b}$$

$$\gamma_{rt} = \frac{1}{r}\frac{\partial u}{\partial\theta} + \frac{\partial v}{\partial r} - \frac{v}{r} \tag{3c}$$

According to the principle of superposition, the general solution of thermal stress consists of two parts:

$$\sigma_r = \sigma_r^0 + \sigma_r^T \tag{4a}$$

$$\sigma_t = \sigma_t^0 + \sigma_t^T \tag{4b}$$

$$\tau_{rt} = \tau^0{rt} + \tau_{rt}^T \tag{4c}$$

Here we define stress function ϕ° and displacement potential function ψ^T respectively:

$$\sigma_r^0 = \frac{1}{r}\frac{\partial\phi^0}{\partial r} + \frac{1}{r^2}\frac{\partial^2\phi^2}{\partial\theta^2} \tag{5a}$$

$$\sigma_t^0 = \frac{\partial^2\phi^0}{\partial r^2} \tag{5b}$$

$$\tau_{rt}^0 = -\frac{1}{r}\frac{\partial^2\phi^0}{\partial r\partial\theta} + \frac{1}{r^2}\frac{\partial\phi^0}{\partial\theta} \tag{5c}$$

and

$$u^T = \frac{\partial\psi^T}{\partial r} \tag{6a}$$

$$v^T = \frac{1}{r}\frac{\partial\psi^T}{\partial\theta} \tag{6b}$$

From (6a) and (6b) we have

$$\sigma_r^T = -\frac{E}{(1+\nu)}\left[\frac{1}{r}\frac{\partial\psi^T}{\partial r} + \frac{1}{r^2}\frac{\partial^2\psi^T}{\partial\theta^2}\right] \tag{7a}$$

$$\sigma_t^T = -\frac{E}{(1+\nu)}\cdot\frac{\partial^2\psi^T}{\partial r^2} \tag{7b}$$

$$\sigma_{rt}^T = \frac{E}{1+\nu}\cdot\left[\frac{1}{r}\frac{\partial^2\psi^T}{\partial r\partial\theta} - \frac{1}{r^2}\frac{\partial\psi^T}{\partial\theta}\right]. \tag{7c}$$

After a lengthy and tedious deduction, we obtain

$$\Delta(\Delta\phi^0) = 0 \tag{8}$$

and for the problem of plane stress, ψ^T meets

$$\Delta\psi^T = (1+\nu)\alpha T(r,\theta), \tag{9}$$

where

$$\Delta = \frac{\partial^2}{\partial r^2} + \frac{1}{r}\frac{\partial}{\partial r} + \frac{1}{r^2}\frac{\partial^2}{\partial\theta^2}.$$

Hence, it is only necessary to solute ϕ° from formula (8) and ψ^T from (9). So we define (8) and (9) as basic equations and their solutions as basic solutions.

2.3 Basic Solutions

We suppose that the thermal stress field has a definition only in a simply connected region involving in origin ($r = 0$). So the thermal stress must satisfy the bounded conditions at origin, from (8) we have [4]

$$\phi^0 = C_{01}r^2 + S_{01}r^2\theta + C_{11}r^3\cos(\theta) + S_{11}r^3\sin(\theta)$$
$$+ \sum_{m=2}(C_{m1}r^{m+2} + C_{m2}r^m)\cos(m\theta)$$
$$+ \sum_{m=2}(S_{m1}r^{m+2} + S_{m2}r^m)\sin(m\theta) \qquad (10)$$

here, $C_{01}, S_{01}, C_{11}, S_{11}, C_{m1}, S_{m1}$ and S_{m2} are also constants.

Now, we apply the Fourier series method to deal with the the solution of ψ^T. Based on the boundary condition (1a) and (1b), we can expand $T(r,\theta)$ to Fourier series.

$$T(r,\theta) = \begin{cases} T_0(r) + \sum_{m=1}\left[T_{cm}(r)\cos(m\theta) + T_{sm}(r)\sin(m\theta)\right], & r \le a \\ 0 & r > a \end{cases} \qquad (11)$$

where $T_0(r)$, $T_{cm}(r)$ and $T_{sm}(r)$ are Fourier coefficients of function $T(r,\theta)$. These coefficients have nothing to do with variable θ, and we assume the solution of ψ^T to be

$$\psi^T = \psi_0^T(r) + \sum_{m=1}\left[\psi_{cm}^T(r)\cos(m\theta) + \psi_{sm}^T(r)\sin(m\theta)\right]. \qquad (12)$$

Substitution of (11) and (12) into (9) gives the solution of ψ^T:

$$\psi^T = (1+\nu)\alpha\int_a^r(\ell n(r) - \ell n(s))\,s\,T_0(s)\,ds$$
$$+ \frac{\alpha}{2}(1+\nu)\sum_{m=1}\frac{1}{m}\left[\int_a^r(r^m - s^{2m}r^{-m})s^{1-m}\,T_{cm}(s)\,ds\right]\cos(m\theta)$$
$$+ \frac{\alpha}{2}(1+\nu)\sum_{m=1}\frac{1}{m}\left[\int_a^r(r^m - s^{2m}r^{-m})s^{1-m}\,T_{sm}(s)\,ds\right]\sin(m\theta). \qquad (13)$$

Up to now, we have obtained the basic solutions.

2.4 Thermal Stress Solution

From (4), (5), (7), (10) and (13), we have:

$$\sigma_r = 2C_{01} + 2S_{01}\theta + 2C_{11}r\cos(\theta) + 2S_{11}r\sin(\theta) - \frac{\alpha E}{r^2}\int_a^r s\,T_0(s)\,ds$$
$$- \frac{\alpha E}{r^3}\cos(\theta)\int_a^r s^2T_{c1}(s)\,ds - \frac{\alpha E}{r^3}\sin(\theta)\int_a^r s^2T_{s1}(s)\,ds$$
$$+ \sum_{m=2}D_{cm}(r)\cos(m\theta) + \sum_{m=2}D_{sm}(r)\sin(m\theta) \qquad (14a)$$

$$\sigma_t = 2C_{01} + 2S_{01} + 6C_{11}r\cos(\theta) + 6S_{11}r\sin(\theta)$$
$$+ \frac{\alpha E}{r^2}\int_a^r s\,T_0(s)\,ds - \alpha E\,T(r,\theta)$$
$$+ \frac{\alpha E}{r^3}\cos(\theta)\int_a^r s^2\,T_{c1}(s)\,ds + \frac{\alpha E}{r^3}\sin(\theta)\int_a^r s^2\,T_{s1}(s)\,ds$$
$$+ \sum_{m=2}E_{cm}(r)\cos(m\theta) + \sum_{m=2}E_{sm}(r)\sin(m\theta) \qquad (14b)$$

$$\tau_{rt} = -S_{01} + 2C_{11}\,r\sin(\theta) - 2\,S_{11}\,r\cos(\theta)$$
$$- \frac{\alpha E}{r^3}\sin(\theta)\int_a^r s^2\,T_{c1}(s)\,ds + \frac{\alpha E}{r^3}\cos(\theta)\int_a^r s^2\,T_{s1}(s)\,ds$$
$$+ \sum_{m=2}F_{cm}(r)\cos(m\theta) + \sum_{m=2}F_{sm}(r)\sin(m\theta) \qquad (14c)$$

where

$$D_{cm} = (m+2-m^2)C_{m1}r^m + (m-m^2)C_{m2}r^{m-2}$$
$$+ \frac{\alpha E}{2}\int_a^r\left[(m-1)r^{m-2} - (m+1)s^{2m}r^{-m-2}\right]s^{1-m}T_{cm}(s)\,ds$$
$$D_{sm} = (m+2-m^2)s_{m1}r^m + (m-m^2)s_{m2}r^{m-2}$$
$$+ \frac{\alpha E}{2}\int_a^r\left[(m-1)r^{m-2} - (m+1)s^{2m}r^{-m-2}\right]s^{1-m}\,T_{sm}(s)\,ds$$
$$E_{cm} = (m+2)(m+1)C_{cm}r^m + m(m-1)C_{m2}r^{m-2}$$
$$- \frac{\alpha E}{2}\int_a^r\left[(m-1)r^{m-2} - (m+1)s^{2m}r^{-m-2}\right]s^{1-m}\,T_{cm}(s)\,ds$$
$$E_{sm} = (m+2)(m+1)s_{m1}r^m + m(m-1)s_{m2}r^{m-2}$$
$$- \frac{\alpha E}{2}\int_a^r\left[(m-1)r^{m-2} - (m+1)s^{2m}r^{-m-2}\right]s^{1-m}\,T_{sm}(s)\,ds$$
$$F_{cm} = -m(m+1)s_{m1}r^m - m(m-1)s_{m2}r^{m-2}$$
$$+ \frac{\alpha E}{2}\int_a^2\left[(m-1)r^{m-2} + (m+1)s^{2m}r^{-m-2}\right]s^{1-m}\,T_{sm}(s)\,ds$$
$$F_{sm} = m(m+1)C_{m1}r^m + m(m-1)C_{m2}r^{m-2}$$
$$- \frac{\alpha E}{2}\int_a^r\left[(m-1)r^{m-2} + (m+1)s^{2m}r^{-m-2}\right]s^{1-m}\,T_{cm}(s)\,ds.$$

Then substitute (14a), (14b) and (14c) into (2a), (2b) and (2c), we can get the solution of corresponding thermal strain immediately. This solution should satisfy stress boundary condition.

On a similar plan, we can also get the solution of the plane strain problem only replacing ν by $\frac{\nu}{1-\nu}$, E by $E/(1-\nu)$ and α by $(1+\nu)\alpha$ separately.

3. MODEL OF VARIATE TEMPERATURE FIELD IN BOZHONG AREA

3.1 The Isotherm Shape Beneath Crust or Upper Mantle Normal Cross Section

After analyzing the data of geologic and tectonic features, seismic wave velocity, geomagnetic anomaly and gravity anomaly, and so on, in Bohai area, we can set up a model to describe isotherm shape like an ellipse with a long axis striking NNE if we cross a normal section from depth 14 to 35 km arbitrarily (Fig.2). There are some ample evidences for our doing so.

(a) Research results [5] of crustal tectonic feature indicates that isobaths of Moho and C discontinuities are all like an ellipse along NNE direction for their long axis, and the depth of inner isobaths is smaller than outer contours. This result perhaps is deeply related to uplifted upper mantle acted by heat substance. So we can consider that the corresponding temperature of inner isothermal line is higher than of outer when we take a fixed normal cross-section, i.e. the isotherm shape is similar to that of isobath.

(b) Seismic tomography technique [6] shows that the isovelocity line of seismic wave is also roughly an ellipse with a long axis striking NNE in depth 14 km. The value of inner isovelocity line is smaller than of outer. This result also accords with the conjecture that the temperature of inner isotherm line is higher.

(c) There are some other evidences about that upper mantle uplifted gradually in Bozhong area , such as the analysis of curie isothermal plane [7] the geological tectonic and the density of upper mantle in Northern China [8]. These evidences also support the isotherm model which we set up.

3.2 The Corresponding Model of Variate Temperature Field

Generally, the VTF is different from the thermal field, but from the isotherm model, we can find the contour model of iso-VTF (see the solid line in Fig.2). In fact, the course of gradually uplifting upper mantle can be considered as equivalent to that of isotherm's spreading along its normal direction [9]. So we can equate the temperature gradient field in a fixed geological age with VTF $T(r,\theta)$ changing with geologic age [10]. In Fig.2, it is few and far between contour lines of VTF along the long axis direction of isotherm ellipse, the temperature gradient is small. In other words, it is more concentrated along the short axis direction of isotherm ellipse, the temperature gradient is bigger. So we can also consider the isoline of VTF as an ellipse, but its long axis strikes NWW and coincides with the short axis of isotherm ellipse.

In the light of the data of Moho discontinuity, the uplift centre locates at about $N\ 38.8°$, $E\ 119.2°$, in Bozhong area, the depth is 3 km shallower than of the boundary belt. Generally, the research demonstrates that the temperature value is about going up $3°C$ to $4°$ along with going down 100 m depth. Accordingly, we consider that the value of the centre place of VTF equals $100°C$. So theoretical formula of our model can be described as follows:

$$T(r,\theta) = \begin{cases} 100(1 - r^2/a^2) + 50(r/a - r^2/a^2)\cos(2\theta) & r \le a \\ 0 & r > a\,. \end{cases} \quad (15)$$

Here, the origin of polar coordinate system locates at $N\ 38.8°$, $E\ 119.2°$. The direction of polar coordinate axis is about along $N\ 45°\ W$, it coincides with the ellipse long axis of VTF (Fig.2). Some evidences indicate that the distance is about 100 km long from the centre place to the boundary belt of uplifted upper mantle, so a = 100 km here.

It is in the range of 9 and 16 km for focal depth of Bohai event [11], and about 15 km for Tangshan event [12]. These results are all in the range of depth 14 and 35 km. Accordingly, the method used to study the distribution of thermal stress is helpful for us to find out the stress feature of Bohai and Tangshan area and the cause of the both earthquakes.

4. THERMAL STRESS FIELD IN BOZHONG AREA AND ITS EFFECT ON BOHAI AND TANGSHAN LARGE EARTHQUAKES

4.1 Computing Result of Thermal Stress Field

Because of the lack of practice data, we simplify the boundary condition as

$$\begin{cases} \sigma_r|_{r=R} = 0 \\ \tau_{rt}|_{r=R} = 0 \end{cases} \quad (16)$$

here $R \gg a$, and R = 400 km in numerical computing.

Substitution of (15) into (14a), (14b) and (14c) separately, we have:

(a) for the district $r \le a$:

$$\begin{aligned} \sigma_r &= -25\alpha E(2 - r^2/a^2 - a^2/R^2) - 50\alpha E[1/4 - r/(5a) - a^4/(20R^4)]\cos(2\theta) \\ \sigma_t &= -25\alpha E(2 - 3r^2/a^2 - a^2/R^2) \\ &\quad - 50\alpha E[-1/4 - 4r/(5a) + r^2/a^2 + a^4/(20R^4) - a^4r^2/(15R^6)]\cos(2\theta) \\ \tau_{rt} &= 50\alpha E[1/4 - 4r/(5a) + r^2/(2a^2) - a^4/(20R^4) + a^4r^2/(10R^6)]\sin(2\theta) \end{aligned} \quad (17)$$

(b) for the district $r > a$:

$$\begin{aligned} \sigma_r &= -25\alpha Ea^2(1/r^2 - 1/R^2) - (5\alpha Ea^4/2)(1/r^4 - 1/R^4)\cos(2\theta) \\ \sigma_t &= 25\alpha Ea^2(1/r^2 + 1/R^2) - 10\alpha Ea^4[1/(4r^4) - 1/(4R^4) + 2r^2/(3R^6)]\cos(2\theta) \\ \tau_{rt} &= -(5a\alpha Ea^4/2)(1/r^4 + 1/R^4 - 2r^2/R^6)\sin(2\theta) \end{aligned} \quad (18)$$

Refer to related data of lithosphere feature, here we choose $\alpha = 3 \times 10^{-5}/°C$ and $E = 8.3 \times 10^{10}\ N/m^2$, then substitute both a = 100 km and R = 400 km into (17) and (18), and get the distributions of σ_r, σ_t and τ_{rt}, versus variable r for some fixed θ. At the same time, we compute the distribution of the maximum value of thermal plane shear stress (MVTPSS) τ_{max} versus r and θ respectively according to the following formula:

$$\tau_{max} = [0.25(\sigma_r - \sigma_t)^2 + \tau_{rt}^2]^{1/2}.$$

These computing results are all seen in Fig.4 besides function $T(r, \sigma)$.

From Fig.4, we can get some conclusions. When θ is fixed, σ_r is of a pressure stress continuously, its value changes from about -10^8 P_a to zero along with variable r increasing from 0 to 400 km successfully. Meanwhile, σ_t shows both pressure and stretching feature with different value of variable r, it changes from about -10^8 to 10^8 P_a along with from centre place to thermal boundary, and then it begins to descend when r gets on an increase. Comparatively, the change of shear stress τ_{rt} can be neglected. On the other hand, σ_r, σ_t and τ_{rt} also change along with variable θ (see Figs.4a, 4b, 4c and 4d).

We specially pay attention to MVTPSS τ_{max} in Fig.4. It changes with r when θ is fixed and goes up to maximum value round the thermal boundary belt. The τ_{max} also changes with θ when r is fixed. For example, assuming r = 100 km, $\tau_{max} \approx 7 \times 10^7$ P_a at $\theta = 0$ or π, $\tau_{max} \approx 5 \times 10^7$ P_a at $\theta = \pi/2$ or $3\pi/2$, so τ_{max} changes within 5×10^7 and 7×10^7 P_a when θ changes (see Fig.5).

4.2 Thermal Stress Field in Bohai and Tangshan Area and its Effect on Bohai and Tangshan Large Earthquakes

Fig.6 demonstrates a plane distribution drawing of MVTPSS τ_{max}. Here we encircle two regions where τ_{max} is greater than 6×10^7 P_a in dash line. In contrast to Fig.2, the two regions almost locate at both ends of long axis of the VTF model. Fig.7 shows the mainly fracture zones and epicenters of earthquakes occurred from January 1900 to July 1976 ($M \geq 3.5$) in Bohai and Tangshan area. Since most earthquakes occurred in the two regions, especially Bohai large earthquake locates on the edge of one region and Tangshan large event within another, so their occurrence can be related reasonably with the thermal stress computed above.

Some data demonstrate that there are many stretching fractures in neighbouring of thermal boundary belt caused by heat uplift [13]. Our result shows that σ_t is of stretching nature, and it comes up to maximum value round the thermal boundary belt. So this result can be related with the emergence or extension of these stretching fracture, and it is a possible reason that middle or small size earthquakes occurred so frequently in the two regions [14], [15].

5. PROBLEM AND DISCUSSION

The thermal model made in this paper is quite simple. It only stresses the ellipse distribution in the centre place of uplifted upper mantle, and with the increase of variable r this ellipse distribution tends to a circle distribution and an absolutely circle at r = 100 km. Moreover, because of the lack of actual data, the stress boundary condition is also simplified greatly as zero at r = 400 km. These simplifications lead to a rather regular distribution of thermal stress field even if we have made a number of improvements on our thermal model. If adequate data are available, the results will be more satisfactory.

Since we only take account of thermal stress in our model, our study is imperfect in the cause of earthquakes in Bozhong area. Tectonic stress should be included in our problem, and it will be considered in the next paper.

Acknowledgments

One of the authors (Z.H.) would like to thank Professor Abdus Salam, the International Atomic Energy Agency and UNESCO for hospitality at the International Centre for Theoretical Physics, Trieste, Italy. The authors would like to thank Professors G. Furlan and Panza in Trieste, and Mr. Lizhixiong at USTC in China for their helpful discussions.

REFERENCES

[1] Zhang Zhili et al., "Influences of the cross inhomogeneous on stress field in crust", *Science in China*, September (1980) Vol.9 (in Chinese).

[2] Zhang Zhili, "Research on the source of stress of Tangshan earthquake", Seism. Jnl. February (1985) Vol.7, No.7 (in Chinese).

[3] R.B. Steven et al., "Thermoelastic stress: How important as a cause of earthquake in Young ocean lithosphere?" J.G.R. **B12** (1985) Vol.90.

[4] Wang Longfu, *Elasticity Theory* (Science Press, 1975) (in Chinese).

[5] Li Jiliang et al., "On the formation and evolution of Bohai Sea", from *The Formation and Evolution of Fault Block in Northern China Region* (Science Press, 1982) (in Chinese).

[6] Liu Futian et al., "Seismic tomography of Northern China Region, Acta Geophys. Sinica, September (1986) Vol.29 (in Chinese).

[7] Hao Shujian and Wang Chunhua, "On the analysis of Curie isothermal surface over the Bohai Sea water area", March (1982) Vol.5 No.1 (in Chinese).

[8] Feng Rui et al., "Combined research on the lithosphere tectonic of Northern China Region", Science Bulletin (1987) Vol.22 (in Chinese).

[9] R.B. Steven et al., "The evolution of impact basins: Cooling, subsidence and thermal stress", J.G.R. **B11** (1985) Vol.90, 12415–12433.

[10] Fu Chenyi et al., *Geophysics* (Science Press, 1985) (in Chinese).

[11] Zhou Huilan et al., Discussion on the focal depth of Bohai earthquake in line with the method of $T_{1/2}$ and V_{max}, Earthquake Research in China (in press).

[12] Zhou Huilan et al., "Some earthquake features at shallow strike-slip focal", Acta Geophys. Sinica (1985) Vol.28, No.6.

[13] Wei Dongping and Zhou Huilan, "Overview of studying thermal stress", Translated World Seismology and Geology (1988) Vol.2.

[14] Gu Gongxu et al., *The Earthquakes catalogue occurred in China* (Science Press, 1984).

[15] Xu Yiujian et al., *Geologic Model and Large Earthquakes' Migration in Northern China* (Science Press, 1986).

FIGURE CAPTIONS

Fig.1 Polar coordinate system and boundaries.
S': Thermal boundary, S: Stress boundary.

Fig.2 Thermal model of uplifted upper mantle in Bozhong area (dash line: contour of equal temperature, solid line: contour of changed field of temperature).

Fig.3 Crustal tectonic feature in Bohai and its neighbouring area.

Fig.4 Distribution of $\sigma_r, \sigma_t, \tau_{rt}, \tau_{max}$ and $T(r, \theta)$, versus variable r.

Fig.5 Distribution curve of τ_{max} versus θ.

Fig.6 Distribution scheme of τ_{max}.

Fig.7 Scheme of mainly fracture zones and epicenter distribution in Bohai and Tangshan area. (January, 1900 – July 1976, $M \geq 3.5$)
(1) Bozhong fault
(2) Bozhong–Yantai–Tranjin fault
(3) Taian–Liaodong fault
(4) Qinghuangdao–Lüshun fault
(5) Changyi–Dadian fault
(6) Cangdong fault
(7) Yanbei fault.

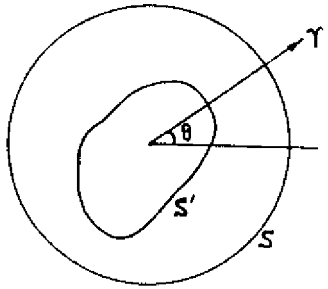

Fig.1

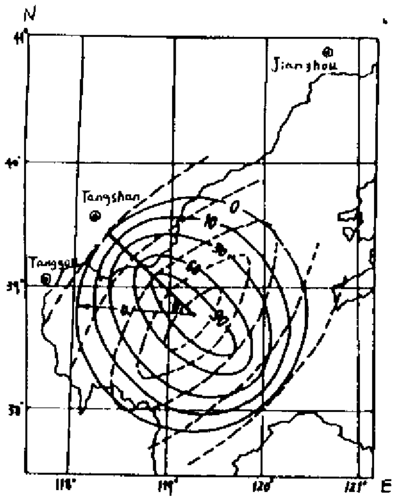

Fig.2

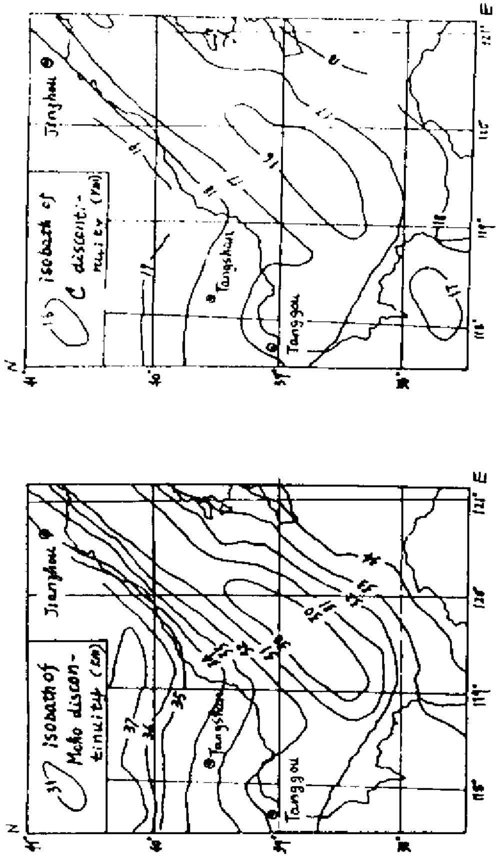

Isobath of Moho discontinuity (km)
Tangshan
Tanggou
(a)
(b)

Fig.3

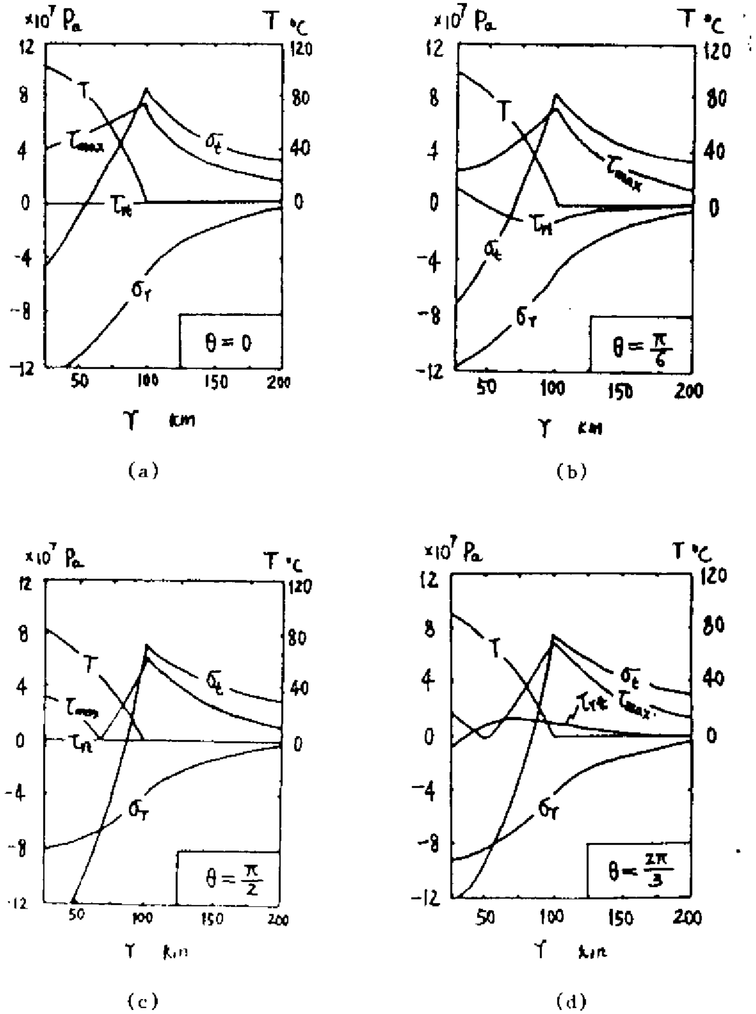

×10^7 Pa
T °C
T
τmax
τrt
σt
σr
θ = 0
θ = π/6
θ = π/2
θ = 2π/3
r km
(a)
(b)
(c)
(d)

Fig.4

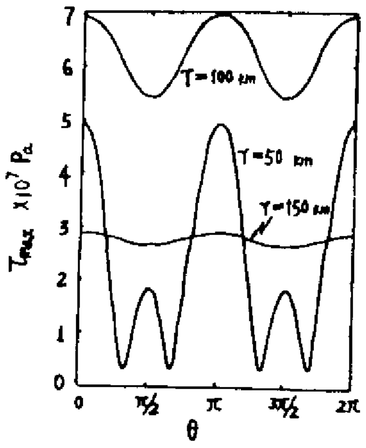

Fig.5

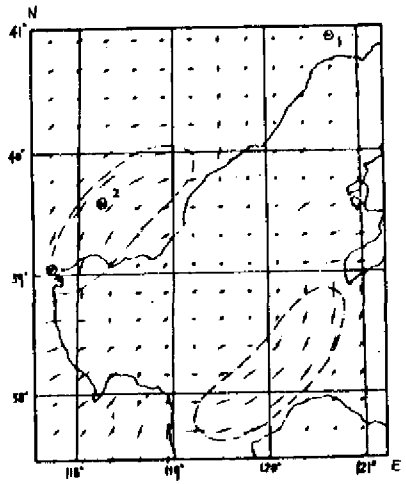

⊙ 1-Jianzhou, 2-Tangshan, 3-Tanggou

Fig.6

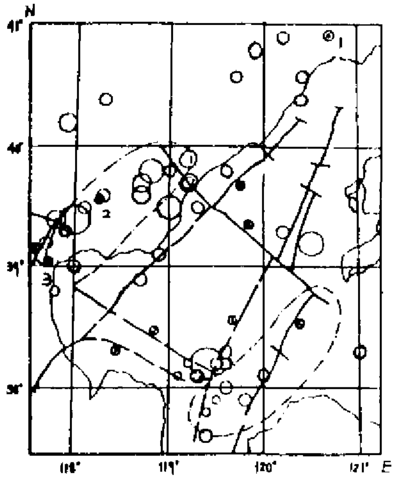

⊙ 1-Jianzhou, 2-Tangshan, 3- Tanggou

Fig.7